Clays and Clay Minerals, Vol. 67, No. 6:507–517, 2019

CRYSTALLIZATION VARIATIONS IN CLAY MINERALS WITH LATITUDE IN JILIN PROVINCE, CHINA: A CLIMATE PERSPECTIVE

Yating Chen[1], Qing Wang[1]*, Yan Han[1], Mengxia Han[1], Jiejie Shen[1], Yuanyuan Kong[2], and Xudong Zhang[3]

[1]College of Construction Engineering, Jilin University, Changchun 130026, People's Republic of China
[2]School of Highway, Chang'an University, Xi'an 710064, People's Republic of China
[3]Department of Civil Engineering, Shanghai University, Shanghai 200444, People's Republic of China

Abstract—In the soils of western Jilin Province in northeastern China, some significant gaps have been observed between the fraction of the soil existing as clay-size particles (<0.002 mm) and the amount attributable to crystalline clay minerals, and that the relative proportions of crystalline clay minerals to the total clay-size fraction (*CP*) apparently varies with latitude. The purpose of the present study was to identify the reason for this discrepancy and to explain the dependence on latitude. The grain sizes and mineral compositions of the whole soils from western Jilin Province, China, were analyzed by laser particle-size analysis (LPSA) and X-ray diffraction (XRD), and the <0.002 mm particle-size fraction was analyzed by XRD and X-ray fluorescence (XRF). The results confirmed that the percentage gaps between the clay fraction and clay minerals increased with increasing latitude. The theoretical illite percentage calculated from K_2O content was compared with the illite percentage measured by XRD, and the results suggested that the measured illite accounted for only a small proportion of the theoretical illite. Structures of some special minerals below the identification threshold of XRD was suggested to be the reason for the percent gaps. The grain size and mineral crystallization both changed with latitude: the soil particle size and the *CP* decreased. In addition, clay minerals were more sensitive to climate than particle sizes were, and the *CP* of clay minerals in the soils within 0~180 cm depth all decreased with increasing latitude; however, the grain size showed patterns with latitude only in relatively shallow soil layers. The present study provides a reference and error analysis for the testing of clay minerals in alpine regions, and more suitable methods may be considered for development of clay-mineral testing in future studies.

Keywords—Clay fraction · Clay minerals · Climate · Crystallization proportion · Western Jilin

INTRODUCTION

Clay minerals are phyllosilicates with extremely fine crystals (generally <0.002 mm in size). Because of their sensitivity to the environment, clay minerals are of great geological significance and are used to study climates and environments during and after soil formation (Thompson et al. 2006). Much effort has been devoted to investigating the factors which indicate the functions of clay minerals in terms of the environment (Środoń 1984; Hunziker et al. 1986). Temperature and precipitation are considered to be vital climatic factors (Thiry 2000). Moreover, some factors, such as the flow rate (Righi & Meunier 1995), vegetation coverage, and organic matter content (Egli et al. 2008), have also proven to be factors that affect clay minerals. Chemical weathering has been suggested to be the link between clay minerals and environmental issues (Egli et al. 2001). Every factor that can affect chemical weathering has an indirect effect on clay minerals; e.g. higher temperature can theoretically increase the rate of chemical weathering (Muhs et al. 2001; Rech et al. 2001), high rainfall also promotes greater chemical weathering (Muhs et al. 2001), and increased freeze-thaw cycles and wetting-drying cycles can contribute to the rate of weathering (Cooper 1960). Characterization of minerals is the first and crucial step for studies on clay minerals. X-ray diffraction (XRD) is the most commonly utilized tool for the analysis of clay minerals, including type, content, and crystallinity. The spatial lattices of mineral crystals are used as XRD gratings, and the direction of X-ray diffraction is related only to the shape and size of unit cells in the crystal structure (Moore & Reynolds Jr 1989). Therefore, each mineral has its own crystal structure and forms a unique diffraction pattern. The crystal-plane spacing calculated from a diffraction peak can be used to distinguish mineral types and infer the percentage of clay minerals semi-quantitatively (Zhang 1990). However, some interference factors, such as types of defects, variable chemical composition, preferred orientation, and structural disorder and diversity, make the quantitative identification and measurement of clay minerals difficult (Zwell & Danko 1975; Środoń et al. 2001; Środoń 2002; Bergaya & Lagaly 2006). A well known example is Huang diffuse scattering (HDS), which is caused by lattice defects or exogenous impurities in the mineral crystal lattice when an X-ray passes through. Therefore, the identification of mineralogy by XRD is usually qualitative (identification) or semi-quantitative. An approach combined with chemical elemental analysis is much more useful to quantify mineralogy, and the most common technique for such determination in rocks and soils is X-ray fluorescence (XRF) (Hupp & Donovan 2018). The electron transition in the atom under radiation is the basis of XRF, so the identification accuracy for elements is high, and XRF precision can reach ±0.01% or even lower. The concentrations of elements are reported in the form of major and minor oxides. The oxides can be used to

* E-mail address of corresponding author: wangqing@jlu.edu.cn
DOI: 10.1007/s42860-019-00048-7

estimate the types of minerals in the rocks or soils based on the chemical formulae of the minerals, which is the way XRF helps to support the identification of XRD results. Among the oxides, K_2O is an important index and indicates the presence of illite. The percent of K_2O in illite is ~6–9%, and other minerals containing K_2O are K-feldspar (16.9%) and mica (11.8%). To remove interference from other minerals, XRF is often conducted on the clay fraction (particle size <0.002 mm) because soil particles smaller than 0.002 mm are almost entirely composed of clay minerals. The classification criterion of <0.005 mm for the clay fraction is used frequently in practical engineering, whereas the <0.002 mm criterion is used more commonly in scientific research; the latter was adopted in the present study.

However, the percentages of the clay fraction (<0.002 mm) and the clay minerals did not match each other from long-term observations on the soils of Jilin Province, China; large clay-fraction percentages corresponded to small clay-mineral percentages in the soils from the study area. Based on these facts, some of the clay particles were assumed in this study to be composed of special clay minerals and that the crystallization of these special clay minerals was too poor to be detected by XRD. The purpose of this study was to test this hypothesis and to identify the origin of the percentage gaps between the clay fraction and the clay minerals content by analyzing grain sizes and mineral compositions of whole samples from the natural soils, using laser particle size analysis (LPSA) and X-ray diffraction (XRD), and then to characterize by XRD, X-ray fluorescence (XRF), and scanning electron microscopy (SEM) the <0.002 mm fraction extracted from the whole soil and to see if comparison of the theoretical and measured illite percentages could explain the gaps.

MATERIALS AND METHODS

Study Area and Soil Properties

The study area, western Jilin in northeast China, is an area distributed with patches of saline soil which, typically, is also frozen seasonally. The area lies in the lowland of the Songnen Plain, near the south-central Songliao Basin (Fig. 1). The Songliao Basin is surrounded by the Greater Khingan with elevations of 1200–1600 m in the west, the Lesser Khingan with elevations of 500–800 m in the northeast, and the Zhangguangcai Mountains (a branch of the Changbai mountains) with an elevation of 1000 m in the east. During the Variscan orogeny, large-scale tectonic faulting formed the initial Songliao depression, and magmatic activity led to extensive intrusion of granitic magma in the Greater Khingan. Mountains of the Greater Khingan and the Changbai continued to rise during the Yanshanian movement, contributing to the further subsidence of the Songliao Basin (Bian et al. 2008). Much weathered debris coming from the surrounding mountains, therefore, accumulated within the basin and provided the initial source of salt in the Songliao Basin. The tectonic activity described above had a significant influence on sedimentation in this region. During the crustal depression, fluvial sediments were first deposited at the bottom of the basin in the early Pleistocene, and lacustrine sediments were then deposited after the basin lake formed in the middle Pleistocene; subsequently, the crust was uplifted, and the basin lake contracted in the late Pleistocene; groups of lakes formed, along with many closed and semi-closed rivers. In summary, because of the poor drainage of this low-lying location and the salt supply, soil salinization is increasing yearly (Wang et al. 2004) and has always been a serious problem for agriculture in the study area. In addition, soils in part of the region exhibited obvious dispersion behaviors (Han et al. 2018), raising a series of engineering problems.

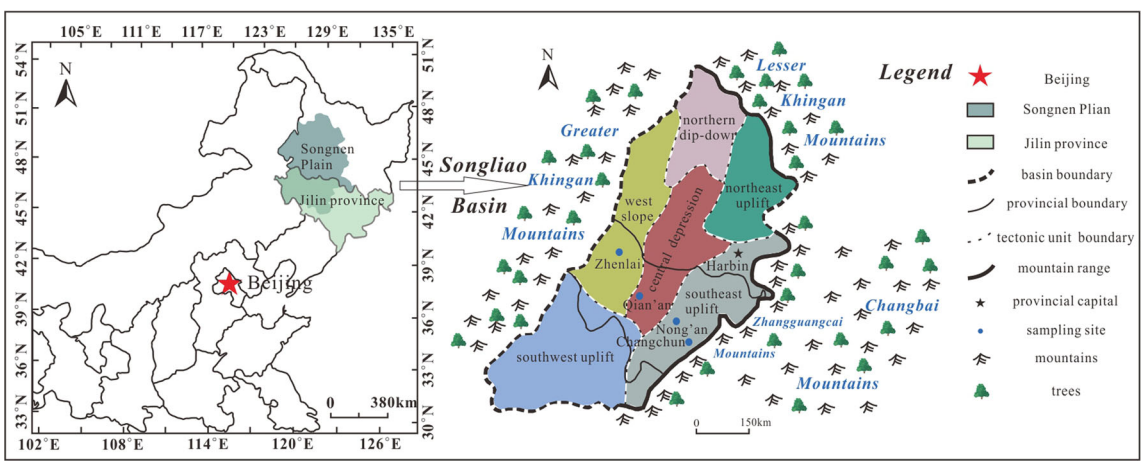

Fig. 1 Geographical locations of the Songliao Basin and study area.

https://doi.org/10.1007/s42860-019-00048-7 Published online by Cambridge University Press

Years of monitoring were conducted at several sampling sites in western Jilin, and the experimental soils for this study were collected from typical saline soil counties at the following geographical coordinates: Nong'an (N44°20′46″; E124°58′07″, elevation 170 m), Qian'an (N45°02′45.49″; E123°47′1.15″, elevation 133 m), and Zhenlai (N45°49′45.50″; E123°16′59.31″, elevation 136 m) (Fig. 1). In addition, data for the loess-like soil in Changchun city (N43°48′59″; E125°19′26″, elevation 222 m) were compared with the test results from the saline soils in order to judge whether the percentage gaps changed with the soil type, which may illustrate the problem better. Loess-like soil in Changchun was formed by alluvial and diluvial processes in the middle and late Pleistocene; it had the typical characteristics of loess but no collapsibility (Wang et al. 1991). Worth mentioning is that the terrain at the sampling sites was relatively flat, so soil erosion was negligible in this study area. Cold and drought characterized the climates in northeast China for years. The average annual evaporation (1698 mm) in western Jilin was roughly three times the precipitation (520 mm) (Han et al. 2018), and the lowest temperature in winter could reach –33°C, influenced by the continental Siberian air mass. At the four sampling sites, monthly minimum temperatures changed over a larger range (approximately –38 to ~11°C) than the range for the monthly maximum temperature (3 to ~40°C) (Fig. 2a). Obvious regularity can be seen (Fig. 2b): the monthly temperature differences at higher latitudes seemed to be larger than those at lower latitudes. Moreover, the average precipitation at lower latitudes was more regular regardless of the month (Fig. 2c). In summary, soils at higher latitudes experienced larger temperature variation, deeper freeze-thaw cycles, and less precipitation. Climates at higher latitudes were much more likely to experience cold and drought than those at the lower latitudes in the study area.

Saline soils used in this study were collected at a depth of 40 cm. The soluble salt content at a depth of 40 cm was the highest in the vertical profile of the superficial soil (Zhang et al. 2017); in addition, salinity varied slightly at a depth of 40 cm among various locations during the same period in the study area. The grain-size distributions of the soils were measured using LPSA (Table 1), and the particles were divided into five ranges: gravel (>2 mm), sand (2–0.075 mm), silt (0.075–0.005 mm), coarse clay (0.005–0.002 mm), and clay (<0.002 mm). Other basic physical-chemical properties of the soils were also found (Table 2). Referring to the USCS (ASTM 2011), the loess-like soil in Changchun and the saline soils in western Jilin can be all classified as lean clay (CL).

Soil Preparation

Soils were divided into two parts for different pretreatments. One part was the natural soil sample used for LPSA (Bettersize2000, Dandong Baite Instrument Co., Ltd., Dandong, China), XRD (Rigaku D/max-2500, Tokyo, Japan), and SEM (JEOL JSM-6700F, Tokyo, Japan). The other part was the clay fraction (<0.002 mm) extracted from the natural soil samples, which was then split into two subsamples for XRD and XRF (ZSX Primus II, Rigaku Corporation, Tokyo, Japan) tests. Clay fractions were extracted according to Stokes' law, and hydrochloric acid (HCl, 0.1 N) and hydrogen peroxide (H_2O_2, 30%) were used to remove the carbonates and organic matter, respectively, from the soils before extraction.

XRD Experiments

X-ray diffraction analysis was conducted on both the natural soils and the clay fraction. Dried samples were crushed and passed through a sieve of 0.075 mm (≈200 mesh) before the XRD and XRF determinations began. Oriented specimens on the glass lens were analyzed by XRD using a CuKα source at 2θ angles from ~3–45° with steps of 0.02°2θ and 2°2θ per min. The patterns were analyzed by comparison with the standard XRD data to determine the mineral types, and the diffraction peaks were used to calculate the mineral content quantitatively. The types and amounts of clay minerals were determined

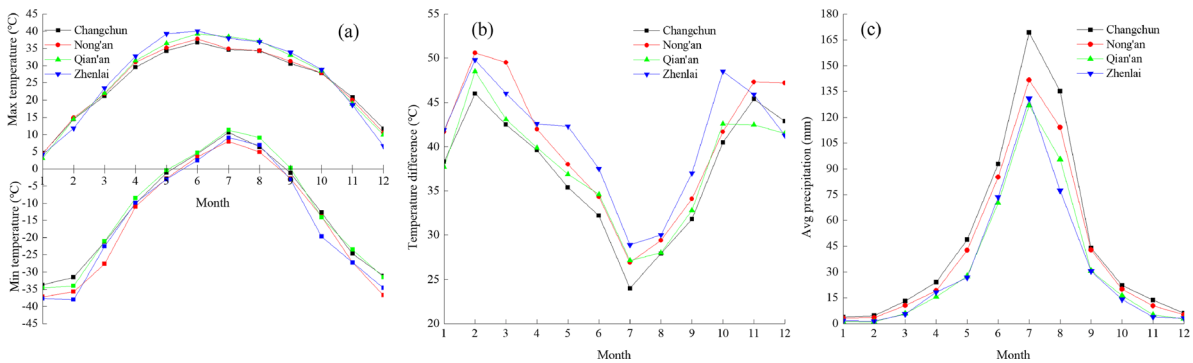

Fig. 2 Monthly average climate information during 1981–2010: (**a**) Maximum and minimum temperatures; (**b**) temperature difference; (**c**) precipitation. (Data collected from the National Meteorological Information Center of China).

https://doi.org/10.1007/s42860-019-00048-7 Published online by Cambridge University Press

Table 1 Grain-size distribution of loess-like soil and saline soils.

Particle size range (mm)	Wt.%			
	Changchun	Nong'an	Qian'an	Zhenlai
>2	0	0	0	0
2–0.075	2.87	3.69	8.74	8.01
0.075–0.005	69.63	53.04	47.46	44.30
0.005–0.002	5.36	8.56	11.06	5.24
<0.002	22.14	34.71	32.74	42.45

quantitatively, principally by the changes in diffraction patterns after some processing. The XRD and LPSA results for natural soil samples were compared with each other to judge the existence of percent age gaps.

X-ray Fluorescence Experiments

X-ray fluorescence was performed on the clay fraction to quantify both major and minor elements. The results of XRF were used to calculate the theoretical minimum illite percent that should be contained in the clay fraction, using illite = 0.09 K_2O.

SEM

Mineral morphologies of the natural soils were examined microscopically by SEM to explain the percentage gaps discovered in this study. Before testing, samples were placed in liquid nitrogen for 30 min for rapid freezing; samples were then vacuum freeze dried using an FD-1A-50 instrument (Beijing Boyikang Experimental Instrument Co., Ltd., Beijing, China) for 8 h to sublimate the ice and, thus, to achieve drying without destruction of the soil structure.

Table 2 Basic physical-chemical properties of the soils.

Property	Changchun	Nong'an	Qian'an	Zhenlai
Plastic limit (%)	23.2	21.3	19.0	20.7
Liquid limit (%)	39.0	41.0	45.8	37.5
Plasticity index	15.8	19.7	26.8	16.8
Total salt content (%)	0.041	1.398	0.710	0.420
Organic matter content (%)	0.62	1.12	0.40	0.23
Classification (USCS)	CL	CL	CL	CL

RESULTS

Grain-size Composition of the Natural Soils

Because the origin of loess-like soil in Changchun was different from that of saline soils in western Jilin, the loess-like soil in Changchun was not involved in the grain-size discussion; it is listed to compare with the mineral composition later. The grain-size distributions of the saline soils at 40 cm (Fig. 3a) depth revealed that the silt group accounted for the largest proportion in soils from different latitudes and this proportion decreased with increasing latitude; meanwhile, the percentage of smaller particles (<0.005 mm) increased with increasing latitude. The test results for particle-size distribution from previous studies are also summarized and plotted together (Fig. 3b-c). Saline soils within ~0–40 cm exhibited the same pattern as that of the soil at 40 cm (Fig. 3b). However, saline soils within 0–180 cm did not have the same patterns as summarized above (the clay group at Qian'an is less prevalent than that at Nong'an in Fig. 3c). Freeze-thaw cycles were considered an important issue influencing the grain-size distribution and degrading the physical and mechanical properties of the rocks and soils (Roman & Ze 2010); the destructive effect of freeze-thaw cycles was greater than those of hot-cold and wet-dry cycles (Khanlari & Abdilor 2015). Soil particles were fragmented stepwise to smaller sizes under these disruptive forces (Wei et al. 2016). From the results, silt particles in the soils at higher latitudes were more likely to be broken into finer particles by stronger physical weathering caused by deeper freeze-thaw cycles than those at lower latitudes. Obviously, the action of 'breaking' was limited by depth. Soils at shallow depths were more influenced by climate than those at greater depths, so the results indicated that climate was likely to be the main factor affecting the size-distribution under the same or a similar geological background. However, the exact depth of influence in the study area cannot be determined to be 40 cm from this study; from the results, one can only say that 40 cm was within the range of influence depths.

Mineral Compositions of the Natural Soils

Quartz and plagioclase were the main nonclay minerals identified in the soils by XRD (Table 3 and Fig. 4); K-feldspar was present over a range of percentages, but no mica was found in the natural soils. Clay minerals were generally scarce in the soils; mixed-layer I-S was most abundant among the clay minerals, followed by illite. The proportions of mixed-layer I-S at lower latitudes were greater because abundant precipitation at low latitudes was good for leaching K^+, thus contributing to the illite-to-smectite transformation (Ren 1988; Hong et al. 2007; Hong 2010). Compared with the particle-size distributions of the soils (Fig. 3a), varying degrees of percentage gaps between the clay fraction and clay minerals could be observed at different latitudes in both the loess-like soil from Changchun and the saline soils from western Jilin.

https://doi.org/10.1007/s42860-019-00048-7 Published online by Cambridge University Press

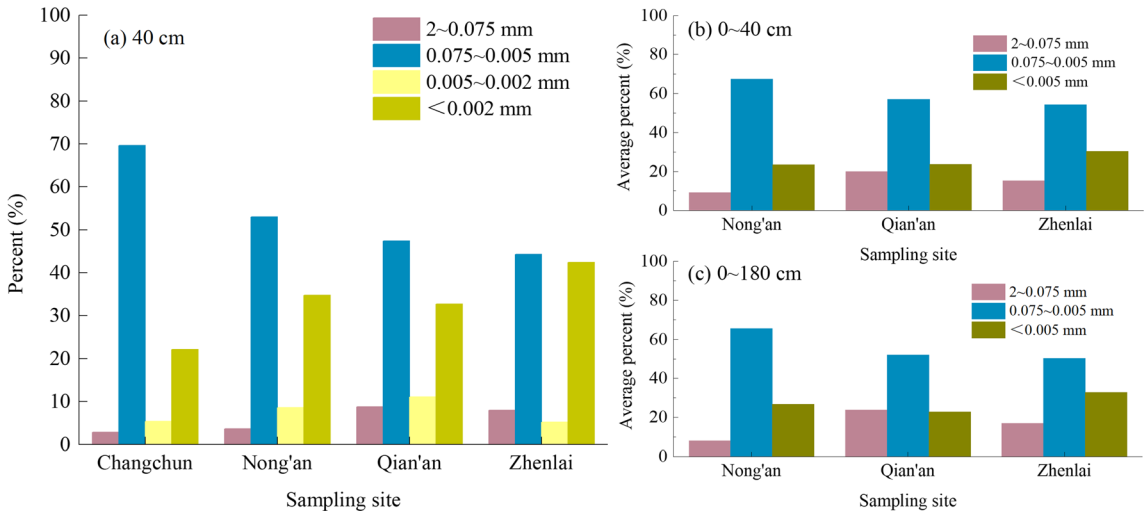

Fig. 3 Grain-size compositions of the soils at or within depths: (**a**) 40 cm, (**b**) 0 to ~40 cm; and (c) 0 to ~180 cm.

Mineral Compositions of the Clay Fraction

Due to unavoidable errors in the extraction process conducted according to Stokes' law, small amounts of non-clay minerals were found in the extracted clay fraction, but clay minerals were absolutely the majority in the clay fraction (Fig. 5a_1, b_1, c_1). Among the clay minerals detected, mixed-layer I-S was still the most common, followed by illite and chlorite (Fig. 5a_2, b_2, c_2). Most of the illite was present in the form of mixed-layer I-S, and the ratio of the mixed layers decreased with latitude, consistent with the results for the natural soils (Fig. 4a-c). In addition, percentages of illite and chlorite, the typical clay minerals in dry and cold environments (Sun et al. 2011), increased with latitude (Fig. 5a_2, b_2, c_2).

Chemical Elemental Oxides of the Clay Fraction

Major and minor elements in the clay fraction were quantified using XRF (Table 4). Due to the presence of K-feldspar in the clay-fraction samples, correction had to be performed by excluding the K_2O from K-feldspar before calculating the theoretical illite percent (Fig. 6a-b). The conversion rate used was the theoretical percentage of 16.9%. The corrected K_2O percent was used to calculate the theoretical illite percent with a conversion rate of 9%; i.e. the theoretical minimum percentage of illite should have existed in the clay fraction (Fig. 6c). The total illite percentage included two types: one type was the illite measured directly by XRD, and the other type was contained in mixed-layer I-S measured by XRD (Fig. 6d). The latter could be calculated by the percentage and ratio of I-S. From the final results (Figs 6c and 6e), the theoretical percentage of illite exceeded the total illite percentage measured by XRD (illite in the form of I-S was also contained in the measurable range (Fig. 6d) in this analysis). This is a semi-quantitative comparison process, and some errors may occur because the K-feldspar and I-S involved in the calculation were obtained from XRD. Other errors may lie in the extraction process for particle sizes of <0.002 mm. However, errors were considered negligible given the large percentage gaps between theoretical and measured illite contents.

Scanning Electron Microscopy Analysis

Illite was the main independent clay mineral in the study area, so illite crystallization, as representative of clay minerals, was examined by SEM (Fig. 7). The crystallinity, microcosmic shape, and thickness of illite are related to their formation mechanisms, such as sedimentary processes and metamorphism. Sedimentary illite has poorer crystallinity than metamorphic illite. In addition, the formation environment can affect the growth of illite structures. OH^- can inhibit growth on the (010) face, leading to relatively faster growth along the [100] direction; this unbalanced growth rate produces more easily illite structures with laths and fibers (Güven 2001). Usually, well crystallized illite exists in the forms of laminated,

Table 3 Mineral composition of loess-like soil in Changchun.

Relative contents of minerals $\omega(B)/10^{-2}$						
Quartz	K-feldspar	Plagioclase	Mixed-layer I-S	Illite	Kaolinite	Chlorite
48	17	18	8	5	3	1

https://doi.org/10.1007/s42860-019-00048-7 Published online by Cambridge University Press

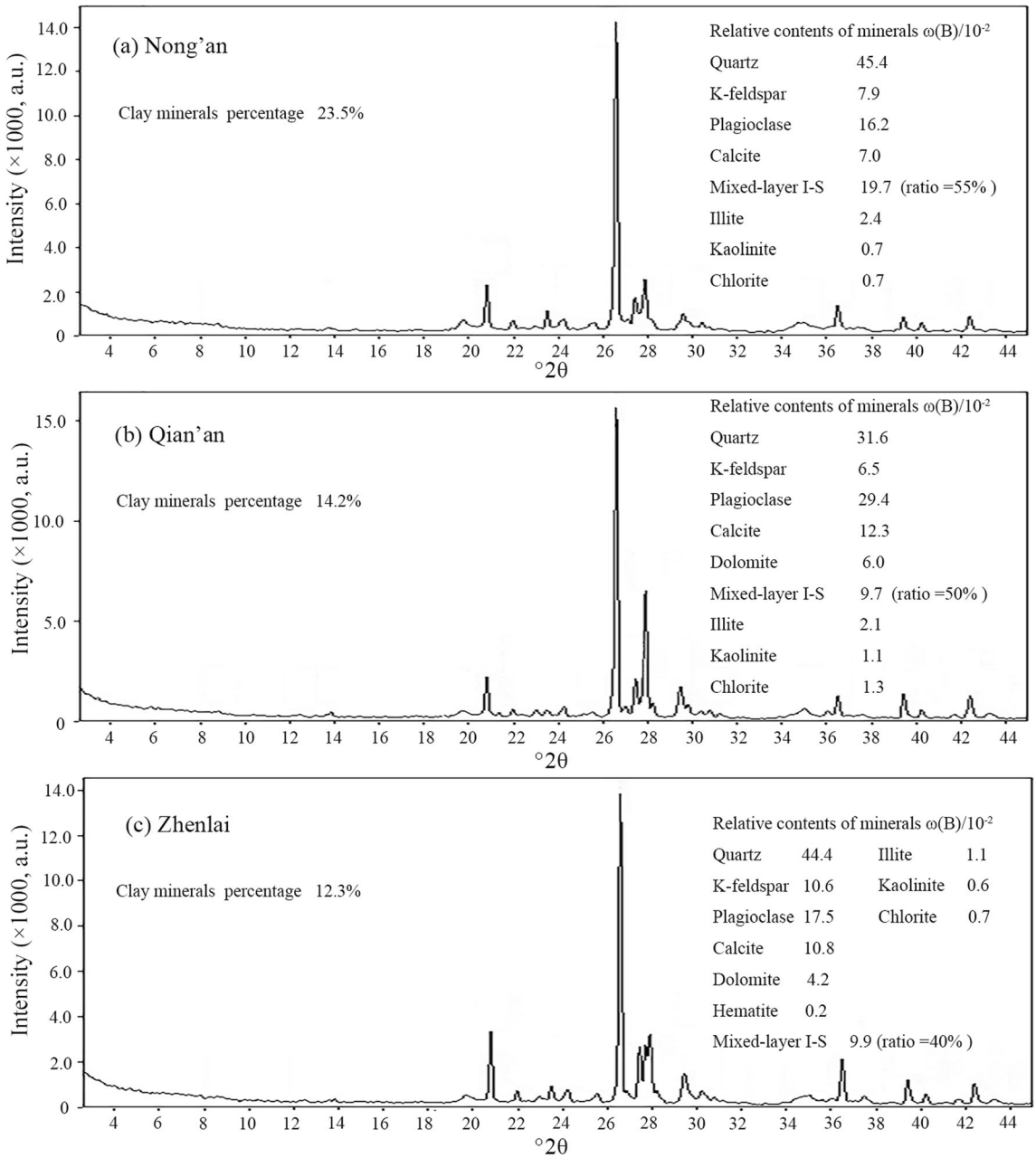

Fig. 4 XRD results of saline soils from various sampling sites: (**a**) Nong'an, (**b**) Qian'an, and (**c**) Zhenlai.

hair-like, and filamentous crystals; when the crystallization is not good enough, illite appears as foliated, tuberculate, or as short fibres. Three stages of illite during the morphological evolution process were proposed by Xing & Xin (1983): microscopically, every stage corresponds to different illite shapes, including foliated lamellar illite (stage I); tuberculate and short fibrous illite (stage II); and laminated, hair-like, and filamentous illite (stage III). Loess-like soil from Changchun showed a flocculated-agglomerate structure (Fig. 7a-b); small laminate illite grains were attached to the particle surfaces, and the edges of illite rolled upward suggesting relatively well crystallized illite (stages II to III) in Changchun. In Nong'an, smaller foliated illite grains were attached to the particle surfaces in a scaly manner. Some or most of the illite edges rolled a little (Fig. 7c). A small number of tuberculate crystals (Fig. 7d) were the prototype of laminate illite; with the improvement

https://doi.org/10.1007/s42860-019-00048-7 Published online by Cambridge University Press

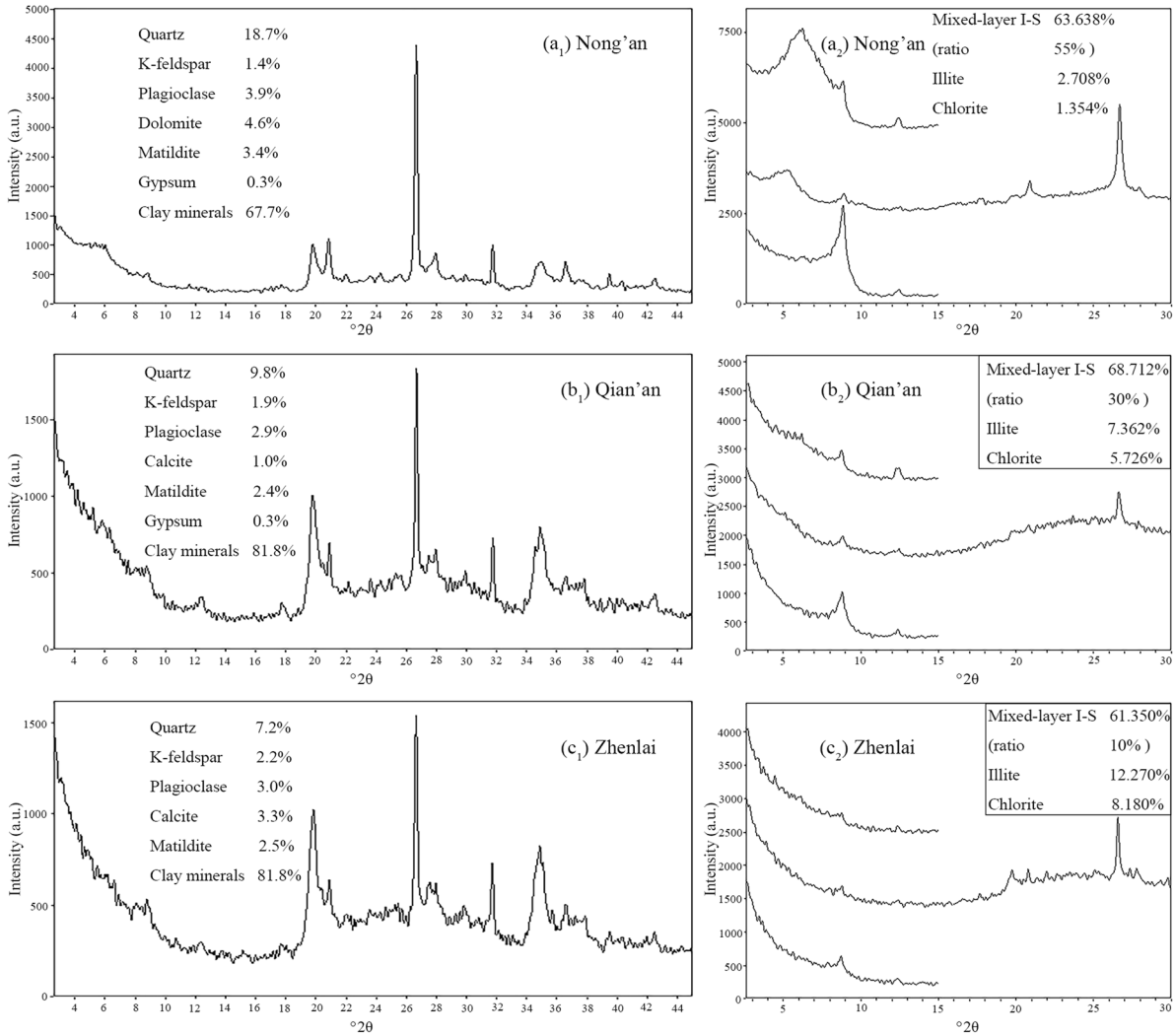

Fig. 5 XRD results of clay fraction from various sampling sites: (a1, b1, c1) clay fraction; (a2, b2, c2) clay minerals in clay fraction.

of crystallization, the tuberculate grains could grow into short fibrous or short laminated grains and finally develop into longer laminated crystals. The SEM results for Nong'an indicated stage I (Fig. 7c) or stage II (Fig. 7d), i.e. not crystallized well enough to reach stage III. The soil structure in Qian'an consisted of alveolate (Fig. 7e-f), ragged, foliated illite attached to honeycomb edges; the crystallization may have represented stage II. In Zhenlai, the soil showed a cotton-like structure (Fig.

Table 4 The types and contents of oxides (wt.%) in soil samples by XRF

Samples												LOI	Sum
	SiO_2	Al_2O_3	Fe_2O_3	FeO	CaO	MgO	K_2O	Na_2O	TiO_2	P_2O_5	MnO		
Nong'an	51.7	15.25	5.33	0.45	2.66	2.77	2.06	2.59	0.56	2.39	0.05	14.02	99.83
Qian'an	45.04	17.31	7.42	0.63	3.22	3.03	2.69	2.18	0.62	3.73	0.08	13.8	99.75
Zhenlai	43.79	15.7	6.87	0.45	3.38	3.77	2.75	2.28	0.54	3.9	0.08	16.22	99.73

https://doi.org/10.1007/s42860-019-00048-7 Published online by Cambridge University Press

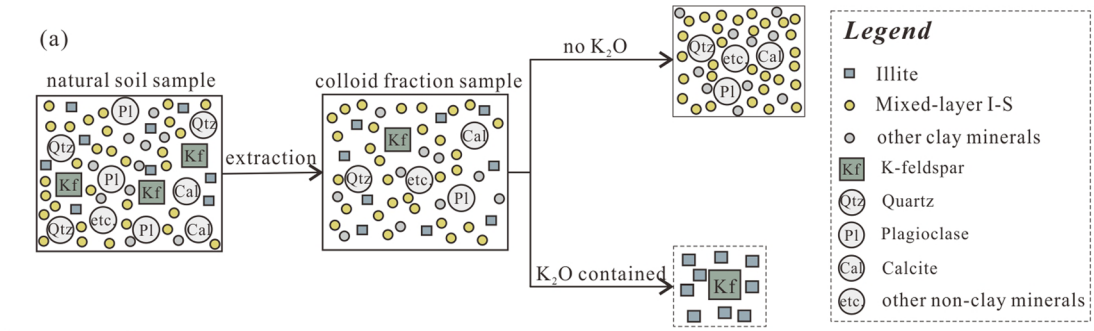

Sampling sites	Percent (%)							
	Total K_2O	K-feldspar	K_2O from K-feldspar	K_2O from illite	Theoretical illite	Illite measured by XRD		Total measured illite
						Illite	Illite contained in I-S	
Nong'an	2.06	1.4	0.2366	1.8234	20.2600	2.708	1.136	3.844
Qian'an	2.69	1.9	0.3211	2.3689	26.3211	7.362	2.217	9.579
Zhenlai	2.75	2.2	0.3718	2.3782	26.4244	12.270	5.577	17.847
			(b)		(c)	(d)		(e)

Fig. 6 Comprehensive analysis of the data for the clay fraction from XRD and XRF: (**a**) Process, (**b**) correction, (**c**) theoretical illite, (**d**) illite measured by XRD, and (**e**) total measured illite.

7g-h); foliated illite grains were small and fragmentary, and their edges (stages I to II) were also roughly curled. In summary, although illite crystallization varied within the study area, not all grains showed good crystallinity.

DISCUSSION

Experimental principles were used to analyze the percentage gaps between the clay fraction and clay minerals, as well as the percentage gaps between theoretical and measured illite. Grain-size testing was obviously based on the size of soil particles; XRF identified the elements by the wavelength or energy of the fluorescence caused by the electron transition under X-ray irradiation; thus, the accuracy and precision were both high. However, XRD distinguished minerals by using spatial lattices of mineral crystals as the gratings; more precisely, XRD measured the mineral structure.

The spacial lattice of the ideal mineral structure has obvious regular and periodic aspects however, due to various types of defects (such as vacancy, dislocation, voids, etc), structural disorder (where part of the structure is not in conformity with the symmetry or periodicity of crystal structure) and diversity (polymorphism caused by the various arrangements of particles), the regular and periodic lattice of mineral structure is destroyed , making it difficult to measure the mineral type accurately. From the test results, some 'special' minerals were suggested by the present authors to exist in the soil; minerals which were <0.002 mm in size and have the characteristics of clay minerals. The 'special' minerals can be detected by LPSA and XRF, therefore. However, these kinds of minerals could not be detected by XRD, possibly because they were amorphous or even absent. The existence of these special minerals with a structure which is below the identification threshold of XRD was suggested to be the reason for the percentage gaps. Minerals with undetectable structures are referred to as the 'poor crystallization problem' in the present study.

The percentage gaps between the clay fraction and clay minerals represented the proportion of poorly crystallized clay minerals in the clay fraction. The crystallization proportion, *CP*, of the clay fraction was calculated using Eq. 1:

$$CP = Mm/Mc \quad (1)$$

where *Mm* is the clay mineral percentage measured by XRD and *Mc* is the clay fraction determined by grain-size experiments. The *CP* of the soil at 40 cm depth showed a decreasing trend with increasing latitude for both the loess-like soil and the saline soils (Fig. 8a); the same regularity also appeared in the saline soils at 0 to ~180 cm (Fig. 8b), although the average particle size did not vary regularly with latitude at 0 to ~180 cm (Fig. 3c). The clay minerals at higher latitudes were more poorly crystallized than those at lower latitudes; the climates at higher latitudes may have inhibited the crystallization of clay minerals. In addition, the influence of climate on crystallization had reached a certain soil depth, as deep as 180 cm (Fig. 8b); however, the influence on particle size was not as deep as 180 cm (Fig. 3c). Clearly, the clay minerals were much more sensitive to climate than the particle sizes were, or chemical weathering proceeded at greater soil depths than was the case for physical weathering.

CONCLUSIONS

The purpose of the present study was to determine the reason why a gap is observed between the clay minerals content and the amount of soil represented by the clay-size fraction in the west Jilin region of northeastern China. Variations with latitude have also been observed. Results from measurements made using LPSA, XRD, XRF, and SEM methods led to the following conclusions:

https://doi.org/10.1007/s42860-019-00048-7 Published online by Cambridge University Press

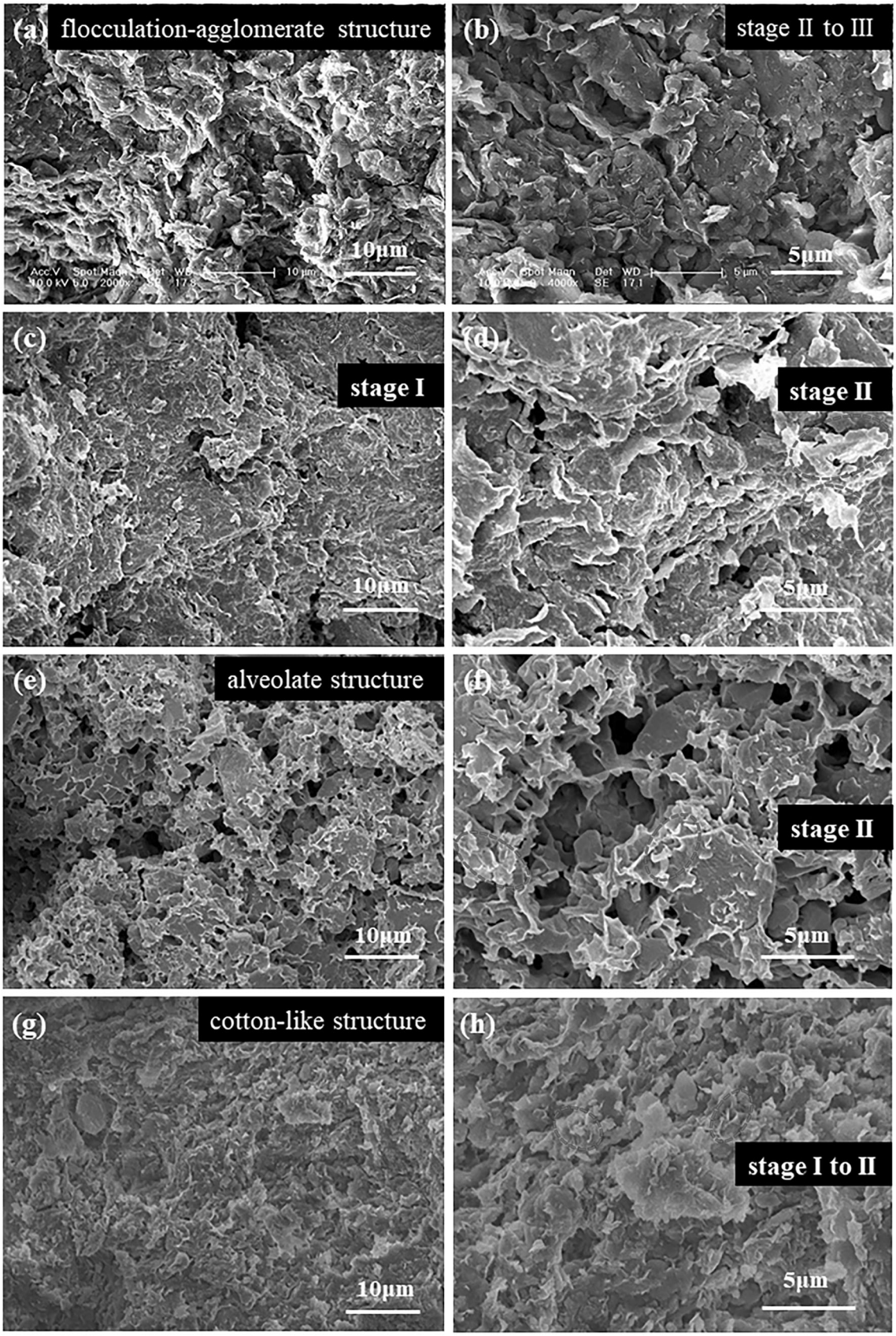

Fig. 7 SEM images of: (**a**, **b**) loess-like soil in Changchun; (**c**, **d**) saline soil in Nong'an; (**e**, **f**) saline soil in Qian'an; and (**g**, **h**) saline soil in Zhenlai.

https://doi.org/10.1007/s42860-019-00048-7 Published online by Cambridge University Press

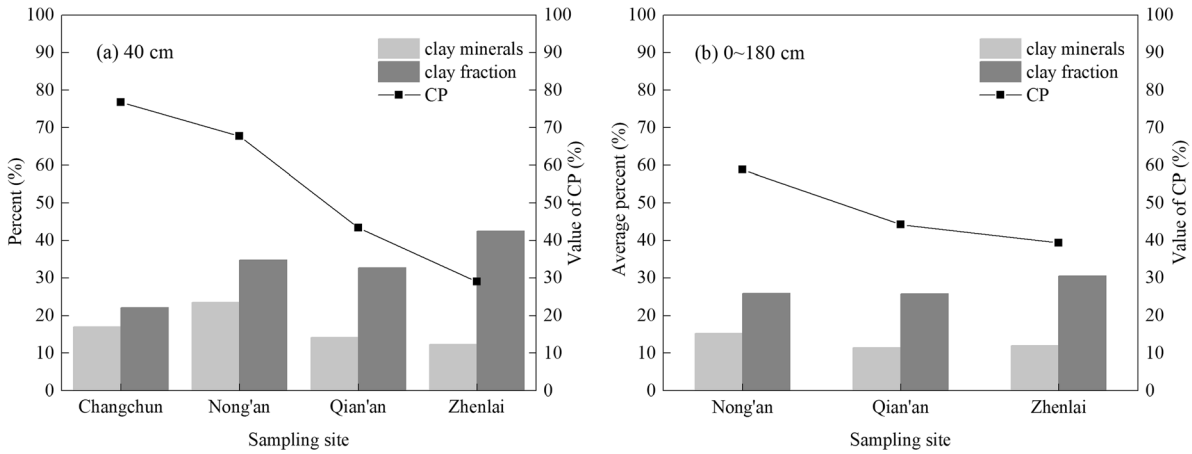

Fig. 8 Clay minerals (wt.%), clay fraction (wt.%), and the values of *CP* at various depths: (**a**) 40 cm, (**b**) 0 to ~180 cm

(1) Within a small geological scale, the regularity of soil particle sizes seemed to be most affected by climate. The silt fraction of saline soils in western Jilin was more likely to be broken into finer particles under the stronger physical weathering caused by the climate at higher latitudes. However, the effect of climate on soil particles was limited by depth, and 40 cm was in the influence range of the climate.

(2) The soils in the study area contained large percentages of clay fractions and small clay mineral percentages. The percentage gap decreased with increasing latitude.

(3) Mixed-layer I-S accounted for the largest proportion of clay minerals in the study area, and the ratio of mixed-layer I-S showed a trend of decreasing with increasing latitude. Most illite existed in the form of I-S, and illite crystallization was mainly poor according to SEM observations.

(4) Significant percentage gaps were also observed between the theoretical illite calculated from K_2O measured by XRF and the illite measured by XRD. The results revealed that the crystallization proportion decreased with latitude. Soils had a larger proportion of non-crystallized clay minerals in their clay fraction at higher latitudes, indicating that the climate at high latitudes may have inhibited mineral crystallization on the whole. Meanwhile, these patterns of crystallization proportion (*CP*) were also reflected in the soils within depths of ~0–180 cm, which suggested that the clay minerals were much more sensitive to climate than the particle sizes were or that chemical weathering had effect in deeper soil layers than was the case for physical weathering.

ACKNOWLEDGMENTS

The authors are grateful for financial support from the Key Program of International (Regional) Cooperation and Exchange of National Natural Science Foundation (Grant No. 41820104001), State Key Program of the National Natural Science Foundation of China (Grant No. 41430642), the Special Fund for Major Scientific Instruments of the National Natural Science Foundation of China (Grant No. 41627801), and the Graduate Innovation Fund of Jilin University (Grant No. 101832018C044). The Editors and anonymous reviewers are thanked for their constructive reviews which helped to improve the manuscript.

REFERENCES

ASTM (2011). *Standard Practice for Classification of Soils for Engineering Purposes (Unified Soil Classification System), D2487-11*. West Conshohocken, Pennsylvania, USA: ASTM International.

Bergaya, F., & Lagaly, G. (2006). Chapter 1: General Introduction: Clays, clay minerals, and clay science. *Developments in Clay Science, 1*, 1–18.

Bian, J. M., Tang, J., & Lin, N. F. (2008). Relationship between saline-alkali soil formation and neotectonic movement in Songnen Plain, China. *Environmental Geology, 55*, 1421–1429.

Cooper, A. W. (1960). An example of the role of microclimate in soil genesis. *Soil Science, 90*, 109–120.

Egli, M., Mirabella, A., & Fitze, P. (2001). Clay mineral formation in soils of two different chronosequences in the Swiss Alps. *Geoderma, 104*, 145–175.

Egli, M., Mirabella, A., & Sartori, G. (2008). The role of climate and vegetation in weathering and clay mineral formation in late Quaternary soils of the Swiss and Italian Alps. *Geomorphology, 102*, 307–324.

Güven, N. (2001). Mica structure and fibrous growth of illite. *Clays and Clay Minerals, 49*, 189–196.

Han, Y., Wang, Q., Kong, Y., Cheng, S., Wang, J., Zhang, X., & Wang, N. (2018). Experiments on the initial freezing point of dispersive saline soil. *Catena, 171*, 681–690.

Hong, H. L. (2010). A review on paleoclimate interpretation of clay minerals. *Geological Science & Technology Information, 29*(*01*), 1–8.

Hong, H. L., Na, Y. U., Xue, H. J., Zhu, Y. H., Xiang, S. Y., & Zhang, K. X. (2007). Clay mineralogy and its palaeoclimatic indicator of the late Pleistocene in Linxia Basin. *Geoscience, 21*, 406–414.

Hunziker, J. C., Frey, M., Clauer, N., Dallmeyer, R. D., Friedrichsen, H., Flehmig, W., Hochstrasser, K., Roggwiler, P., & Schwander, H. (1986). The evolution of illite to muscovite: Mineralogical and isotopic data from the Glarus Alps, Switzerland. *Contributions to Mineralogy & Petrology, 92*, 157–180.

Hupp, B. N., & Donovan, J. J. (2018). Quantitative mineralogy for facies definition in the Marcellus Shale (Appalachian Basin, USA) using XRD-XRF integration. *Sedimentary Geology, 371*, S003707381830112X.

https://doi.org/10.1007/s42860-019-00048-7 Published online by Cambridge University Press

Khanlari, G., & Abdilor, Y. (2015). Influence of wet-dry, freeze-thaw, and heat-cool cycles on the physical and mechanical properties of upper red sandstones in central Iran. *Bulletin of Engineering Geology and the Environment, 74*, 1287–1300.

Moore, D. M., & Reynolds Jr., R. C. (1989). *X-ray Diffraction and the Identification and Analysis of Clay Minerals*. Oxford, UK: Oxford University Press.

Muhs, D. R., Bettis, E. A., Been, J., & McGeehin, J. P. (2001). Impact of climate and parent material on chemical weathering in loess-derived soils of the Mississippi river valley. *Soil Science Society of America Journal, 65*, 1761–1777.

Rech, J. A., Reeves, R. W., & Hendricks, D. M. (2001). The influence of slope aspect on soil weathering processes in the Springerville volcanic field, arizona. *Catena, 43*, 49–62.

Ren, L. (1988). Intermediate structures of clay minerals during transformation. *Acta Sedimentologica Sinica, 6(01)*, 80–87+136.

Righi, D., & Meunier, A. (1995). Origin of clays by rock weathering and soil formation. In B. Velde (Ed.), *Origin and Mineralogy of Clays* (pp. 43–161). Berlin, Heidelberg: Springer.

Roman, L. T., & Ze, Z. (2010). Effect of freezing-thawing on the physico-mechanical properties of a morianic clayey loam. *Soil Mechanics and Foundation Engineering, 47*, 96–101.

Środoń, J. (1984). X-ray powder diffraction identification of illitic materials. *Clays and Clay Minerals, 32*, 337–349.

Środoń, J. (2002). Quantitative mineralogy of sedimentary rocks with emphasis on clays and with applications to K-Ar dating. *Mineralogical Magazine, 66*, 677–688.

Środoń, J., Drits, V. A., McCarty, D. K., Hsieh, J. C. C., & Eberl, D. D. (2001). Quantitative X-ray diffraction analysis of clay-bearing rocks from random preparations. *Clays and Clay Minerals, 49*, 514–528.

Sun, Q. F., Chen, F. H., Christophe, C., & Zhang, J. W. (2011). Application progress of clay minerals in the researches of climate and environment. *Acta Mineralogica Sinica, 31*, 146–152.

Thiry, M. (2000). Palaeoclimatic interpretation of clay minerals in marine deposits: An outlook from the continental origin. *Earth-Science Reviews, 49*, 201–221.

Thompson, A., Chadwick, O. A., Rancourt, D. G., & Chorover, J. (2006). Iron-oxide crystallinity increases during soil redox oscillations. *Geochimica et Cosmochimica Acta, 70*, 1710–1727.

Wang, Q., Chen, J., & Wang, M. (1991). A preliminary study on collapsibility of loess-like soil in Changchun. *Jilin Geology, 3*, 51–56.

Wang, C., Wu, Z., Shi, Y., & Wang, R. (2004). The resource of saline soil in the northeast china. *Chinese Journal of Soil Science, 35*, 643–647.

Wei, Y., Wu, X., Xia, J., Shen, X., & Cai, C. (2016). Variation of soil aggregation along the weathering gradient: Comparison of grain size distribution under different disruptive forces. *Plos One, 11*(*8*), e0160960. https://doi.org/10.1371/journal.pone.0160960.

Xing, S. Q., & Xin, G. Q. (1983). Evolution of crystal morphology of authigeinc illite in sandstone and its geological significance. *Petroleum Exploration and Development, 6*, 17–22.

Zhang, N. X. (1990). *Methods for the Study of Clay Minerals*. Beijing, China: Science Press.

Zhang, X. D., Wang, Q., Huo, Z. S., Yu, T. W., Wang, G., Liu, T. B., & Wang, W. H. (2017). Prediction of frost-heaving behavior of saline soil in western Jilin province, China, by neural network methods. *Mathematical Problems in Engineering*. https://doi.org/10.1155/2017/7689415.

Zwell, L., & Danko, A. W. (1975). Applications of X-ray diffraction methods to quantitative chemical analysis. *Applied Spectroscopy Reviews, 9*, 167–221.

(Received 3 August 2019; revised 25 November 2019; AE: Warren D. Huff)